Magnetic Cooperative Effects in Small Ni–Ru Clusters

ARTICLE *in* THE JOURNAL OF PHYSICAL CHEMISTRY A · DECEMBER 2011

Impact Factor: 2.69 · DOI: 10.1021/jp208802e · Source: PubMed

4 AUTHORS, INCLUDING:

F. Aguilera-Granja
Universidad Autónoma de San Luis Potosí
150 PUBLICATIONS **1,370** CITATIONS
SEE PROFILE

L. J. Gallego
University of Santiago de Compostela
160 PUBLICATIONS **2,402** CITATIONS
SEE PROFILE

Andrés Vega
Universidad de Valladolid
176 PUBLICATIONS **1,952** CITATIONS
SEE PROFILE

THE JOURNAL OF PHYSICAL CHEMISTRY A

ARTICLE

pubs.acs.org/JPCA

Magnetic Cooperative Effects in Small Ni−Ru Clusters

F. Aguilera-Granja,[†] R. C. Longo,[*,‡] L. J. Gallego,[‡] and A. Vega[§]

[†]Instituto de Física "Manuel Sandoval Vallarta", Universidad Autónoma de San Luis Potosí, 78000 San Luis Potosí, México

[‡]Departamento de Física de la Materia Condensada, Facultad de Física, Universidad de Santiago de Compostela, E-15782 Santiago de Compostela, Spain

[§]Departamento de Física Teórica, Atómica y Óptica, Universidad de Valladolid, E-47011 Valladolid, Spain

ABSTRACT: We report ab initio calculations of the structures, magnetic moments, and electronic properties of Ni_7-xRu_x clusters ($x = 0-7$) using a density-functional method that employs linear combinations of pseudoatomic orbitals as basis sets, nonlocal norm-conserving pseudopotentials, and the generalized gradient approximation to exchange and correlation. The pure clusters Ni_7 and Ru_7 were predicted to have octahedral and cubic structures, respectively, and the binary clusters were found to be either decahedral (Ni_6Ru, Ni_5Ru_2, and Ni_4Ru_3) or cubic (Ni_3Ru_4, Ni_2Ru_5, and $NiRu_6$). For Ni_5Ru_2 and Ni_4Ru_3 we found a magnetic cooperative phenomenon, which is due to both geometrical effects and electronic contributions through Ni−Ru hybridization.

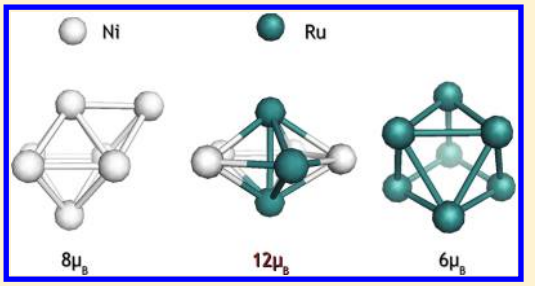

I. INTRODUCTION

The magnetic properties of low-dimensional systems in general and, in particular, of clusters of transition metal (TM) atoms have been the subject of intense research effort for both theoretical reasons (the desire to understand how the magnetic properties change when the dimension of a material is reduced to nanometer length scale) and with a view to the potential technological applications, such as the design of high-density magnetic storage devices (see, e.g., refs 1 and 2). The investigation performed so far on the magnetic properties of homonuclear free-standing TM clusters has produced very interesting results. For instance, it has been shown that the magnetic moments of TM clusters of the 3d ferromagnetic elements Fe, Co, and Ni are significantly larger than the corresponding bulk values[3−8] and that clusters of certain nonmagnetic 4d TMs such as Ru, Rh, and Pd become magnetic.[9−14] The enhanced magnetism at the cluster level can be understood as a consequence of the reduction of the local coordination number, which produces a strong localization of the d-electron states, and a reduction of the effective d band width.

Although less extensive than in the single-component case, investigation has also been performed on the magnetic behavior of TM bimetallic clusters (often referred to as nanoalloys). This kind of system offers the possibility to tailor the magnetic properties through the choice of the component species and the composition, often leading to new magnetic states that are not possible for homonuclear TM clusters. In particular, ultrafine Co−Rh particles with a mean diameter of 1.65 nm, synthesized chemically by a process based on the decomposition in mild conditions of an organometallic precursor in the presence of a stabilizing polymer, have been shown to have a strong increase of the magnetization, up to twice the value of the bulk Co−Rh alloy.[15] This result, which was interpreted as the first evidence of the cooperative role of both alloying and size reduction to the enhanced induced electronic spin polarization of the Rh atoms by the magnetic Co atoms, opened new questions concerning the influence of the size on the magnetism of 3d−4d bimetallic clusters. Small Co_xRh_y clusters ($x + y \leq 4$) were investigated by Dennler et al.[16] by density-functional theory (DFT) calculations using the VASP code[17,18] with the generalized gradient approximation (GGA) to exchange and correlation.[19] The results by Dennler et al. showed that small Co−Rh clusters were magnetic, with average magnetic moments per atom significantly larger than those of bulk alloys of similar compositions, in qualitative keeping with the experimental findings by Zitoun et al.[15] on Co−Rh nanoparticles. Subsequently, Berlanga-Ramírez et al.[20] used a semiempirical aproach which combined the many-body Gupta potential[21] with the tight-binding method[22] to investigate the magnetic properties of Co_xRh_y clusters ($x + y \approx 100$ and $x \approx y$) of different symmetries and chemical orders, showing that, for all the clusters considered, the magnetic moments of the Rh atoms had a strong dependence on the geometrical and chemical environment. In particular, it was found that the Rh atoms close to the Co atoms displayed a noticeable spin polarization induced by the magnetic moments of the surrounding Co atoms and that this 3d−4d cooperative effect worked in conjunction with the surface effect. Cooperative effects have also been predicted in the case of the cluster $Ni_{12}Rh$.[23] However, in spite of these and other studies in the area, further investigations are still necessary for satisfactory understanding of the magnetic behavior of 3d−4d bimetallic clusters in general.

Received: September 12, 2011
Revised: October 20, 2011
Published: October 27, 2011

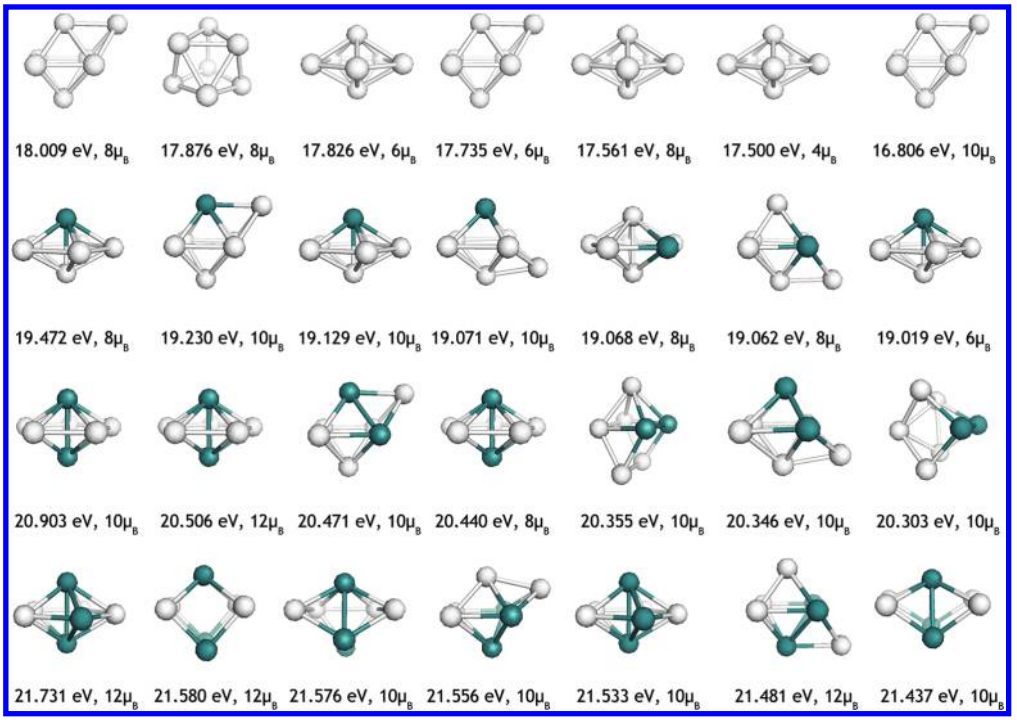

Figure 1. First lowest energy isomers found for $Ni_{7-x}Ru_x$ clusters ($x = 0-3$) with their total binding energies and total spin magnetic moments. White spheres represent Ni atoms and blue spheres Ru atoms.

In the work described here we perform extensive ab initio DFT calculations to investigate possible cooperative effects in the binary clusters Ni_7-xRu_x ($x = 0-7$). Several properties of this kind of cluster have in recent years been investigated, including its catalytic activity when supported on appropriate substrates (see, e.g., ref 24). However, to our knowledge, there have hitherto been no systematic studies on their structural, electronic, and magnetic properties, even for the smaller species, as reported in this paper. The essential technical details of the computational method used are sketched in section II, our results are discussed in section III, and in section IV we summarize our main conclusions.

II. DETAILS OF THE COMPUTATIONAL PROCEDURE

Our calculations were performed using the SIESTA code,[25] which solves the single-particle Kohn−Sham equations using numerical pseudoatomic orbitals as basis sets. For the exchange and correlation potential we used the Perdew−Burke−Ernzerhof form of the GGA.[26] The atomic cores were replaced by nonlocal norm-conserving Troullier−Martins pseudopotentials[27] factorized in the Kleinman−Bylander form[28] and included nonlinear core corrections. The pseudopotentials for Ni and Ru were generated using the valence configurations $4s^1 3d^9$ and $5s^1 4d^7$, respectively. Valence states were described using double-ζ doubly polarized basis sets. The energy cutoff used to define the real-space grid for the numerical calculations involving the electron density was 250 Ry. Tests performed with a bigger energy cutoff gave virtually the same results.

In the calculations the clusters were placed in a supercell of size $20 \times 20 \times 20$ Å^3, large enough for interaction between the cluster and its replicas in neighboring cells to be negligible and for it to suffice to consider only the Γ point ($k = 0$) when integrating over the Brillouin zone. We considered starting geometries of octahedral, decahedral, and cubic types. For each binary cluster (of fixed geometry and stoichiometry) we analyzed all the possible homotops, i.e., all the possible locations of the two types of atoms among the sites of the cluster, and a large number of (collinear) starting configurations of the atomic spin magnetic moments. The forces on ions were computed using a variant of the Hellmann−Feynman theorem that includes Pulay-type corrections to take into account that the basis sets are not complete and move with the atoms.[25] Using a conjugate gradient method,[29] all the structures were relaxed without any symmetry or spin constraints (except for the assumption of magnetic collinearity) until interatomic forces were smaller than 0.006 eV/Å. The binding energies of the clusters were computed as the sign-reversed total energies relative to the same number of isolated atoms.

Due to the extensive exploration performed of the clusters potential energy surfaces we can reasonably assume that the isomer of lowest energy identified in our calculations for each cluster corresponds to its ground state. The reliability of our results is also supported by careful selection of all the ingredients used in our SIESTA calculations: basis sets, energy cutoff, forces convergence criterion, etc.

III. RESULTS AND DISCUSSION

Figures 1 and 2 show the structures, binding energies, and total spin magnetic moments μ (in units of the Bohr magneton, μ_B) of the seven first lowest energy isomers found in our calculations for each $Ni_{7-x}Ru_x$ cluster ($x = 0 - 7$). Specific results for the ground-state clusters (i.e., the most stable isomers) are given in Figure 3, which shows the magnetic moments per atom, the average interatomic distances r, and the values of the chemical short-range order parameter σ, defined as $\sigma = (N_{Ni-Ni} + N_{Ru-Ru} - N_{Ni-Ru})/(N_{Ni-Ni} + N_{Ru-Ru} + N_{Ni-Ru})$, where N_{ij} is the number of nearest-neighbor ij pairs. Table 1 contains all the relevant geometric and

dx.doi.org/10.1021/jp208802e |J. Phys. Chem. A 2011, 115, 13950–13955

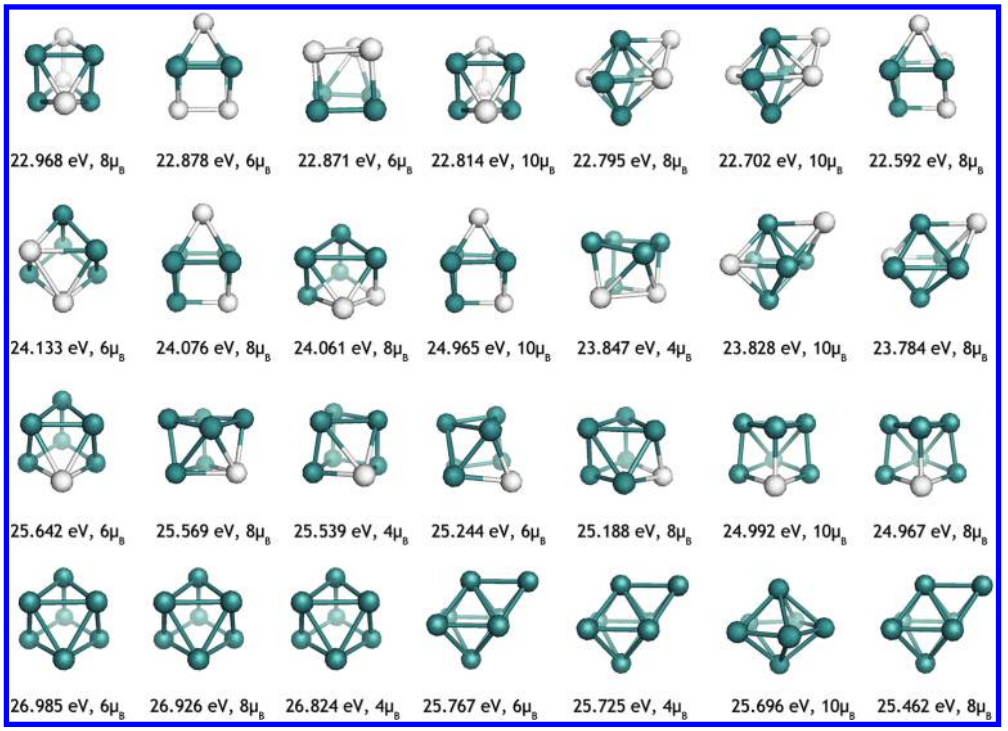

Figure 2. As for Figure 1 but for $x = 4-7$.

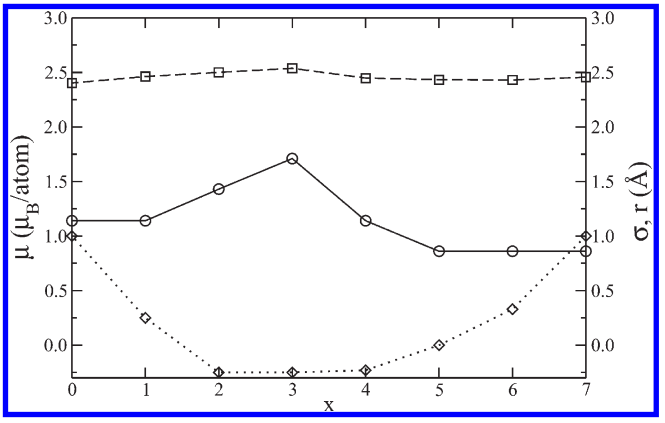

Figure 3. Magnetic moments per atom μ (circles), average interatomic distances r (squares), and values of the order parameter σ (diamonds) of the ground-state clusters $Ni_{7-x}Ru_x$ ($x = 0-7$) plotted against x. Lines joining points are merely visual aids.

magnetic information derived from our calculations for these ground-state clusters.

The predicted ground-state structures of the pure clusters Ni_7 and Ru_7, a capped octahedron with $\mu = 8\ \mu_B$ and a cubic-like structure with $\mu = 6\ \mu_B$, are in keeping with the results obtained by Xie et al.,[30] Bae et al.,[31] and Lu et al.[32] using different DFT methods (note that, as in the study performed by Bae et al.,[31] the change in energy necessary for reaching a spin isomer of the ground-state cluster Ru_7 is very small, in contrast to the behavior of Ni_7). When increasing the x concentration starting from $x = 0$, there are two structural transitions: one from the octahedral to the decahedral structure, which occurs at $x = 1$, and the other from the decahedral to the cubic structure, which occurs at $x = 4$. The chemical short-range order parameter σ, introduced by

Table 1. Structures, Average Interatomic Distances (in Angstroms), and Total and Partial Magnetic Moments (in μ_B/atom) of the Ground-State Clusters $Ni_{7-x}Ru_x$ ($x = 0-7$)

x	structure	r	r_{Ni-Ni}	r_{Ru-Ru}	r_{Ni-Ru}	μ	μ_{Ni}	μ_{Ru}
0	octahedral	2.402	2.402			1.14	1.14	
1	decahedral	2.462	2.454		2.474	1.14	0.95	2.30
2	decahedral	2.500	2.490	2.626	2.492	1.43	1.06	2.33
3	decahedral	2.537	2.512	2.647	2.511	1.71	1.08	2.56
4	cubic	2.448	2.333	2.391	2.491	1.14	0.94	1.29
5	cubic	2.433	2.736	2.323	2.473	0.86	0.81	0.88
6	cubic	2.430		2.377	2.535	0.86	1.08	0.82
7	cubic	2.456		2.456		0.86		0.86

Ducastelle,[33] allows one to determine if a certain binary system, in general, has a heterocoordination tendency, i.e., a preference for unlike atom pairs, or a homocoordination tendency. The first case corresponds to positive values of σ and the second case to negative values. Although for small binary clusters it is not always easy to appreciate chemical order effects, it is clear from Figure 3 that at intermediate compositions the binary cluster $Ni_{7-x}Ru_x$ has a tendency to mixing or heterocoordination.

The magnetic moment results of Figure 3 and Table 1 show the existence of cooperative effects in some of these clusters. Specifically, the total magnetic moments of Ni_5Ru_2 and, more markedly, Ni_4Ru_3 are larger than those of the pure Ni_7 and Ru_7 clusters, something that is unexpected since Ru is less magnetic than Ni. In Figure 3 and Table 1 it can also be seen that the average interatomic distance is nearly constant in the whole range of concentrations, although there are slight increases at $x = 2$ and 3, which helps in the enhancement of the magnetic moments in Ni_5Ru_2 and Ni_4Ru_3 due to electron delocalization. However, in spite of this correlation, the increases of the average interatomic

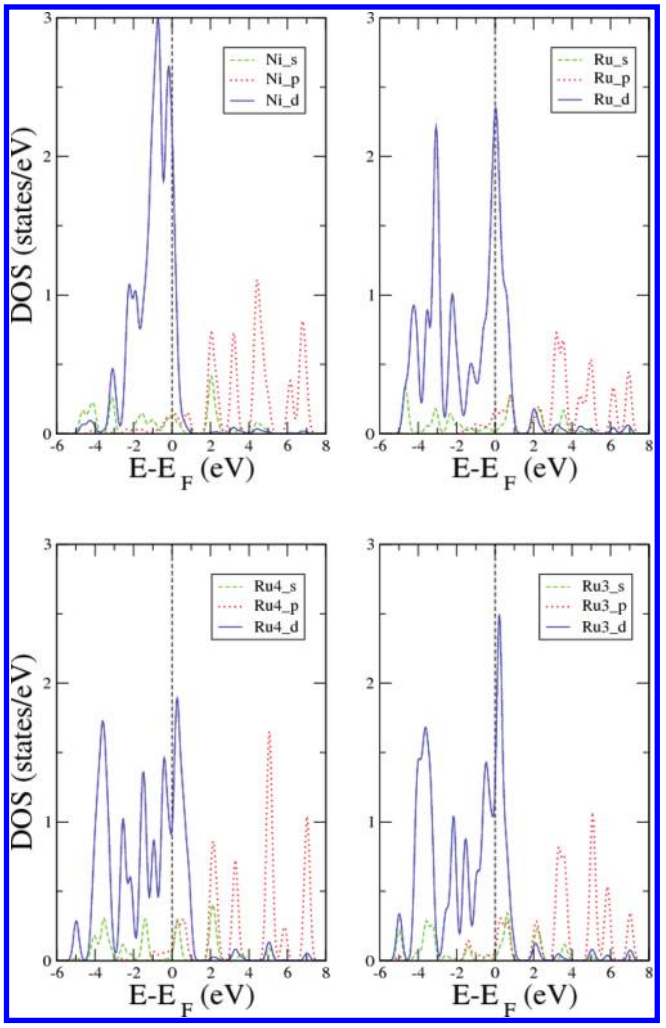

Figure 4. (Top) Paramagnetic DOS of Ni_4Ru_3 projected on the Ni and Ru atoms and the s, p, and d orbitals (dashed green line, dotted red line, and continuous blue line, respectively). (Bottom) Paramagnetic DOS of the decahedral Ru_7 cluster projected on the four Ru atoms located at the same positions as the four Ni atoms in Ni_4Ru_3 and on the remaing Ru atoms as well as on the s, p, and d orbitals (dashed green line, dotted red line, and continuous blue line, respectively). Delta functions composing the projected DOS have been replaced by Gaussian functions of finite breadth.

distance are too small to be the unique reason for the observed magnetic moments of Ni_5Ru_2 and Ni_4Ru_3, so that we have to look for other contributions in order to understand the magnetic cooperative phenomenon. In what follows, we discuss the case of the cluster Ni_4Ru_3 for which the effect is bigger.

The local magnetic moments distribution of the clusters $Ni_{7-x}Ru_x$, shown in Table 1 indicates that the average magnetic moment of the Ni atoms has a nearly constant value of around 1 μ_B for all concentrations (except, evidently, for $x = 7$), while the average magnetic moment of the Ru atoms increases from about 0.86 μ_B, the value for the pure Ru_7 cluster, to 2.56 μ_B, the value for Ni_4Ru_3. Moreover, the increase of the average magnetic moment of the Ru atoms takes place when the cluster loses the cubic symmetry of the pure Ru_7 cluster and adopts the decahedral symmetry, i.e., when it has less than four Ru atoms. This means that, at least in part, the cooperative phenomenon can be attributed to structural effects, i.e., to the structural transition

Table 2. Total and Partial Magnetic Moments (in μ_B/atom) of the Clusters M_4Ru_3 (M = Fe, Co, Pd, Pt, and Ru) with the Decahedral Geometry of the Ground-State Cluster Ni_4Ru_3

M	μ	μ_M	μ_{Ru}
Fe	2.857	3.343	2.210
Co	2.286	2.213	2.383
Pd	1.714	0.828	2.895
Pt	1.714	0.920	2.773
Ru	1.119	0.708	1.664

from the cubic to the decahedral symmetry as decreasing the number of Ru atoms. This is confirmed by the fact that the total magnetic moment of the most stable decahedral isomer of Ru_7 is 10 μ_B, much larger than that of the cubic, ground-state structure, 6 μ_B (Figure 2). This increase of 4 μ_B is, therefore, only due to a symmetry effect. However, it should be noted that the total magnetic moment of Ru_7 in the decahedral isomer is still 2 μ_B smaller than that of Ni_4Ru_3 in its ground state, which has the same symmetry (Figure 1). This is so despite the fact that the magnetic moment per atom of the decahedral cluster Ru_7 (1.43 μ_B) is considerably larger than the average magnetic moment of the Ni atoms in Ni_4Ru_3 (1.08 μ_B). In other words, one would expect that after replacing Ru atoms by Ni atoms in the decahedral cluster Ru_7 the total magnetic moment should decrease, contrary to what happens. Therefore, we have to conclude that besides the geometrical contribution there is also an electronic contribution to the cooperative effect through Ni−Ru hybridization by means of which the Ru atoms close to the Ni atoms in the decahedral cluster Ni_4Ru_3 are able to gain the additional magnetic moment.

In order to clarify how the Ni−Ru hybridization works in favor of increasing the magnetic moment of the Ru atoms in Ni_4Ru_3 and, therefore, the total magnetic moment we analyzed in detail the electronic structure by computing the density of states (DOS). Figure 4 shows the paramagnetic DOS of the decahedral, ground-state cluster Ni_4Ru_3 projected on the Ni and Ru atoms and the paramagnetic DOS of the decahedral Ru_7 cluster projected on the four Ru atoms located at the same positions as the four Ni atoms in Ni_4Ru_3 and on the remaining Ru atoms. Ni−Ru hybridization in Ni_4Ru_3 is reflected in the large degeneracy of the electronic Ru states at the Fermi level (E_F) in the paramagnetic DOS, which does not take place in the pure Ru_7 cluster. According to the Stoner criterion, the Ru atoms close to the Ni atoms have a stronger tendency to be spin polarized than in the pure Ru_7 cluster, and consequently their magnetic moments will be much larger.

The marked peak in the paramagnetic DOS of Ni_4Ru_3 results mainly from the hybridization of the d states of both elements, as is inferred from the orbital projections of the DOS (Figure 4). In order to clarify further the influence of this electronic effect to the increase of the magnetic moment of the cluster Ni_4Ru_3 we also performed SIESTA/GGA calculations for the clusters Fe_4Ru_3 and Co_4Ru_3 with the same decahedral geometry as Ni_4Ru_3, i.e., without relaxation. Our intention was to see if the degree of degeneracy of the Ru d states at the Fermi level due to hybridization (and the concomitant increase of the magnetic moment) was related with the particular band filling of Ni. By putting Fe or Co instead of Ni in the neigborhood of Ru we obtained a lower increase of the Ru magnetic moment (see Table 2). The lower the d-band filling of the element close to Ru, the lower the increase of the Ru magnetic moment. Thus, the

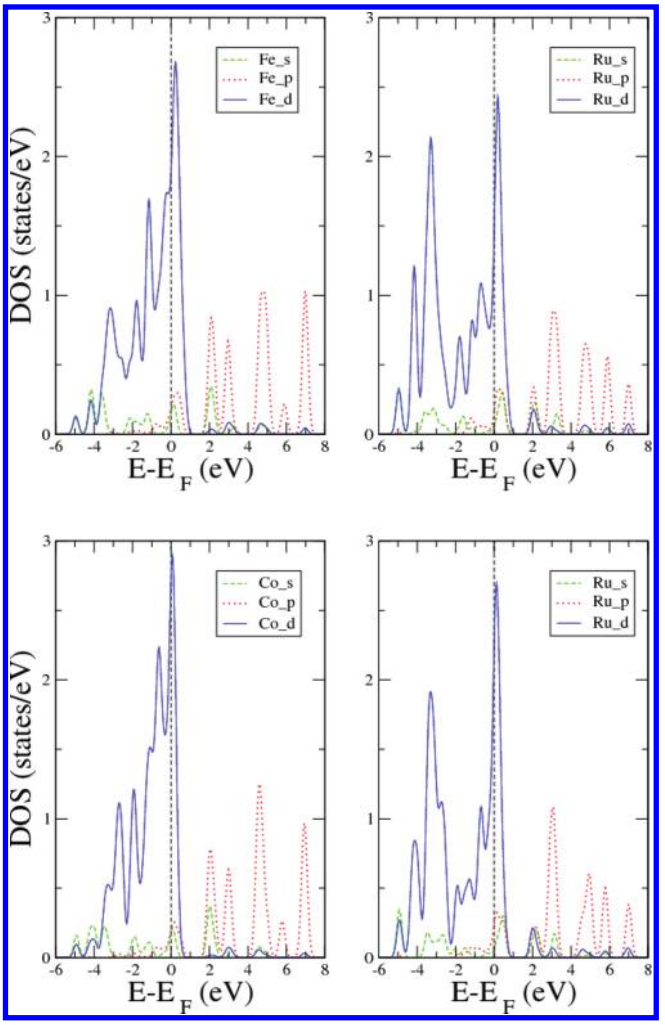

Figure 5. (Top) Paramagnetic DOS of Fe_4Ru_3, with the same decahedral geometry as Ni_4Ru_3, projected on the Fe and Ru atoms and the s, p, and d orbitals (dashed green line, dotted red line, and continuous blue line, respectively). (Bottom) Paramagnetic DOS of Co_4Ru_3, with the same decahedral geometry as Ni_4Ru_3, projected on the Co and Ru atoms and the s, p, and d orbitals (dashed green line, dotted red line, and continuous blue line, respectively). Delta functions composing the projected DOS have been replaced by Gaussian functions of finite breadth.

average Ru magnetic moments of Fe_4Ru_3 and Co_4Ru_3 were 2.21 μ_B and 2.38 μ_B, respectively, while the corresponding value for Ni_4Ru_3 increases up to 2.56 μ_B. This increase of the magnetic moment when going from Fe to Co to Ni is consistent with the Stoner criterion and correlates with the paramagnetic DOS at the Fermi level. If we compare the paramagnetic DOS of Fe_4Ru_3, Co_4Ru_3, and Ni_4Ru_3, all with the same decahedral geometry, the Ru peak of Ni_4Ru_3 at E_F moves gradually to the empty states for Co_4Ru_3 and Fe_4Ru_3 (see Figures 4 and 5), while the value of the DOS at E_F decreases (this value is 2.35, 2.28, and 1.53 states/eV for Ni_4Ru_3, Co_4Ru_3, and Fe_4Ru_3, respectively). Further evidence in favor of our argumentation is that substituting Ni by its isoelectronic elements of the 4d or 5d series (Pd and Pt, respectively) in the decahedral cluster Ni_4Ru_3 gave also a strong increase of the average Ru magnetic moment, while substituting Ni by Ru (isoelectronic with Fe) produced a much smaller increase (see Table 2). Finally, it should be pointed out that the increase of the Ru magnetic moment in the Ni environment is larger than that in the Fe or Co environments, despite the fact that the average magnetic moments of the Fe and Co atoms in Fe_4Ru_3 and Co_4Ru_3, respectively, are considerably larger than that of the Ni atoms in Ni_4Ru_3 (see Tables 1 and 2). This gives further support to our argument based on the hybridization effect, since otherwise a larger increase of the Ru magnetic moment would have been induced in Fe_4Ru_3 and Co_4Ru_3 as a consequence of the local magnetic field produced by the Fe or Co atoms.

We note that spin−orbit coupling (SOC) was not taken into account in our SIESTA/GGA calculations because it is expected to have little influence on the magnetic properties of the clusters considered. Several authors have discussed the effect of the SOC for a variety of 3d, 4d, and 5d TM clusters.[34−37] These studies have shown that the change in the magnetic configuration leads to small geometrical distortions of the cluster structure and that for clusters of a 5d TM like Pt the SOC can be strong enough to change the energetic ordering of the structural isomers, the orbital contribution to the total magnetic moment being comparable to the spin contribution. However, for clusters of 3d and 4d TMs such as Ni and Pd the SOC was found to be much smaller.

In order to estimate the contribution of SOC to the magnetic behavior of Ni−Ru clusters we performed fully self-consistent DFT calculation on the ground-state structure of Ni_4Ru_3, as predicted by SIESTA/GGA, using the plane-wave code VASP,[18,38] which solves the spin-polarized Kohn−Sham equations within the projector-augmented wave method. This allows a considerable efficiency in terms of computational time. As in our SIESTA calculations, for exchange and correlation we used the Perdew−Burke−Ernzerhof form of the GGA.[26] In the absence of SOC, VASP preserved the total spin magnetic moment of Ni_4Ru_3 predicted by SIESTA after the atomic and electronic degrees of freedom were relaxed simultaneously without any symmetry or spin constraint. When the SOC was included, the resulting magnetic moment remained essentially unchanged and the effect on the cluster geometry was negligible (the changes in bond lengths were smaller than 0.01 Å). The easy axis of this particular cluster lies in the equatorial plane, while the hard axis is perpendicular to the equatorial plane, along the apical Ru atoms. To determine these axes, several self-consistent calculations changing the spin quantization axis were required. The magnetic anisotropy energy, calculated as the energy difference between the easy axis and the hard axis configurations, was about 3 meV. We note that this energy barrier is not enough for stabilizing the magnetization against thermal fluctuations (a temperature of 40 K overcomes this energy barrier). The orbital magnetic moments were approximately 0.1 μ_B in the easy axis configuration (those of Ni increased up to 0.18 μ_B in the hard axis configuration, while those of Ru were slightly lower than 0.14 μ_B) and pointed in the same direction as the spin magnetic moments. These results show that SOC effects will not modify the general trends predicted for the Ni−Ru clusters by considering only the dominant spin contribution.

IV. SUMMARY AND CONCLUSIONS

In this paper we performed DFT calculations of the structures, magnetic moments, and electronic properties of $Ni_{7-x}Ru_x$ clusters (x = 0−7) using the code SIESTA,[25] nonlocal norm-conserving pseudopotentials,[27] and the GGA for exchange and

correlation.[26] Appropriate starting geometries (octahedral, decahedral, and cubic), all the possible homotops at each stoichiometry, and, in each case, a large number of spin configurations were considered to obtain the final lowest energy structures and magnetic moments.

The pure ground-state clusters Ni_7 and Ru_7 were predicted to have a capped octahedral geometry with $\mu = 8\,\mu_B$ and a cubic-like structure with $\mu = 6\,\mu_B$, respectively, in keeping with the results obtained by Xie et al.,[30] Bae et al.,[31] and Lu et al.[32] using different DFT methods. For the binary clusters we found that the preferred geometry is decahedral for Ni_6Ru, Ni_5Ru_2, and Ni_4Ru_3 and cubic for Ni_3Ru_4, Ni_2Ru_5, and $NiRu_6$.

The total magnetic moments of Ni_5Ru_2 and, more markedly, Ni_4Ru_3 were found to be noticeably larger than those of the pure Ni_7 and Ru_7 clusters, in spite of Ru being less magnetic than Ni. Electronic structure calculations showed that, together with the geometrical contribution, there is an electronic contribution through Ni−Ru hybridization responsible for this cooperative effect, a behavior which is related to the particular band filling of Ni.

To our knowledge, experimental studies on the magnetic behavior of $Ni_{7-x}Ru_x$ clusters have not yet been carried out. We expect that, when performed, they may confirm the results reported in this paper, particularly the cooperative phenomenon. The predicted enhancement of the magnetic moment of the binary cluster at $x = 3$ ($12\,\mu_B$) makes it potentially useful in recording and storage technologies. Since atomic clusters are generally manipulated not in vacuum but supported on a suitable substrate, it should be interesting to investigate the kind of substrates on which such property is retained. Graphene is probably a good candidate because it has proved to interact weekly with TM nanostructures.[39]

AUTHOR INFORMATION

Corresponding Author

*E-mail: roberto.longo@utdallas.edu.

ACKNOWLEDGMENT

This work was supported by PROMEP-SEP-CA230, México, the Spanish Ministry of Science and Innovation in conjunction with the European Regional Development Fund (Grant Nos. FIS2008-02490/FIS and FIS2008-04894/FIS), the Junta de Castilla y León (Grant VA104A11-2), and the Directorate General for R+D+i of the Xunta de Galicia (Grant No. INCITE09E2R206033ES). Facilities provided by the Centro Nacional de Supercomputo (CNS) from the IPICyT, San Luis Potosí, S.L.P., México, and the Galician Supercomputing Centre (CESGA) are also acknowledged.

REFERENCES

(1) Alonso, J. A. *Chem. Rev.* **2000**, *100*, 637.
(2) Pastor, G. M. *Atomic Clusters and Nanoparticles*; NATO ASI, Les Houches, Sesion LXXIII, EDP Sciences; Guet, C., Hobza, P., Spiegelman, F., David, F., Eds.; Springer, Berlin, 2001, p 335.
(3) Cox, D. M.; Trevor, D. J.; Whetten, R. L.; Rohlfing, E. A.; Kaldor, A. *Phys. Rev. B* **1985**, *32*, 7290.
(4) Bucher, J. P.; Douglass, D. C.; Bloomfield, L. A. *Phys. Rev. Lett.* **1991**, *66*, 3052.
(5) Billas, I. M. L.; Becker, J. A.; Châtelain, A.; de Heer, W. A. *Phys. Rev. Lett.* **1993**, *71*, 4067.
(6) Billas, I. M. L.; Châtelain, A.; de Heer, W. A. *Science* **1994**, *265*, 1682.
(7) Billas, I. M. L.; de Heer, W. A.; Châtelain, A. *J. Non-Cryst. Solids* **1994**, *179*, 316.
(8) Apsel, S. E.; Emmert, J. W.; Deng, J.; Bloomfield, L. A. *Phys. Rev. Lett.* **1996**, *76*, 1441.
(9) Billas, I. M. L.; Châtelain, A.; de Heer, W. A. *J. Magn. Magn. Mater.* **1997**, *168*, 64.
(10) Douglass, D. C.; Bucher, J. P.; Bloomfield, L. A. *Phys. Rev. B* **1992**, *45*, R6341.
(11) Reddy, B. V.; Khanna, S. N.; Dunlap, B. I. *Phys. Rev. Lett.* **1993**, *70*, 3323.
(12) Cox, A. J.; Louderback, J. G.; Bloomfield, L. A. *Phys. Rev. Lett.* **1993**, *71*, 923.
(13) Cox, A. J.; Louderback, J. G.; Apsel, S. E.; Bloomfield, L. A. *Phys. Rev. B* **1994**, *49*, 12295.
(14) Moseler, M.; Häkkinen, H.; Barnett, R. N.; Landman, U. *Phys. Rev. Lett.* **2001**, *86*, 2545.
(15) Zitoun, D.; Respaud, M.; Fromen, M. C.; Casanove, M. J.; Lecante, P.; Amiens, C.; Chaudret, B. *Phys. Rev. Lett.* **2002**, *89*, 037203.
(16) Dennler, S.; Morillo, J.; Pastor, G. M. *Surf. Sci.* **2003**, *532*−*535*, 334.
(17) Kresse, G.; Hafner, J. *Phys. Rev. B* **1993**, *47*, R558.
(18) Kresse, G.; Furthmüller, J. *Phys. Rev. B* **1996**, *54*, 11169.
(19) Perdew, J. P.; Chevary, J. A.; Vosko, S. H.; Jackson, K. A.; Pederson, M. R.; Singh, D. J.; Fiolhais, C. *Phys. Rev. B* **1992**, *46*, 6671.
(20) Berlanga-Ramírez, E. O.; Aguilera-Granja, F.; Montejano-Carrizales, J. M.; Díaz-Ortiz, A.; Michaelian, K.; Vega, A. *Phys. Rev. B* **2004**, *70*, 014410.
(21) Cleri, F.; Rosato, V. *Phys. Rev. B* **1993**, *48*, 22.
(22) Franco, J. A.; Vega, A.; Aguilera-Granja, F. *Phys. Rev. B* **1999**, *60*, 434.
(23) Aguilera-Granja, F.; Longo, R. C.; Gallego, L. J.; Vega, A. *J. Chem. Phys.* **2010**, *132*, 184507.
(24) Crisafulli, C.; Scire, S.; Minico, S.; Solariego, L. *Appl. Catal.* **2002**, *225*, 1.
(25) Soler, J. M.; Artacho, E.; Gale, J. D.; García, A.; Junquera, J.; Ordejón, P.; Sánchez-Portal, D. *J. Phys.: Condens. Matter* **2002**, *14*, 2745.
(26) Perdew, J. P.; Burke, K.; Ernzerhof, M. *Phys. Rev. Lett.* **1996**, *77*, 3865.
(27) Troullier, N.; Martins, J. L. *Phys. Rev. B* **1991**, *43*, 1993.
(28) Kleinman, L.; Bylander, D. M. *Phys. Rev. Lett.* **1982**, *48*, 1425.
(29) Press, W. H.; Teukolsky, S. A.; Vetterling, W. T.; Flannery, B. P. *Numerical Recipes in Fortran*, 2nd ed; Cambridge University Press: Cambridge, 1992.
(30) Xie, Z.; Ma, Q. M.; Liu, Y.; Li, Y. C. *Phys. Lett. A* **2005**, *342*, 459.
(31) Bae, Y. C.; Osanai, H.; Kumar, V.; Kawazoe, Y. *Mater. Trans.* **2005**, *46*, 159.
(32) Lu, Q. L.; Luo, Q. Q.; Chen, L. L.; Wan, J. G. *Eur. Phys. J. D* **2011**, *61*, 389.
(33) Ducastelle, F. *Order and Phase Stability in Alloys*; Elsevier: New York, 1991.
(34) Huda, M. N.; Niranjan, M. K.; Sahu, B. R.; Kleinman, L. *Phys. Rev. A* **2006**, *73*, 053201.
(35) Fernández-Seivane, L.; Ferrer, J. *Phys. Rev. Lett.* **2007**, *99*, 183401.
(36) Bloński, P.; Dennler, S.; Hafner, J. *J. Chem. Phys.* **2011**, *134*, 034107.
(37) Bloński, P.; Hafner, J. *J. Phys.: Condens. Matter* **2011**, *23*, 136001.
(38) Kresse, G.; Joubert, D. *Phys. Rev. B* **1999**, *59*, 1758.
(39) Johll, H.; Kang, H. C.; Tok, E. S. *Phys. Rev. B* **2009**, *79*, 245416.